

Wideband frequency-reconfigurable antenna for sub-6 GHz wireless communication

Tejal Tandel¹, Samir Trapasiya²

¹Department of Electronics Engineering, Madhuben and Bhanubhai Institute of Technology (MBIT), School of Engineering, CVM University, Gujarat, India

²Department of Electronics and Communication Engineering, G H Patel College of Engineering and Technology (GCET), CVM University, Gujarat, India

Article Info

Article history:

Received Jun 11, 2025

Revised Sep 2, 2025

Accepted Oct 9, 2025

Keywords:

5G network

Advance design system simulation

Compact

PIN diode

Reconfigurable antenna

ABSTRACT

This paper presents a compact dual-band frequency-reconfigurable monopole antenna for sub-6 GHz wireless applications. Using a single PIN diode, the antenna switches between 2.7 GHz and 3.9 GHz bands, achieving bandwidths of 472 MHz and 1130 MHz, respectively, with peak gains up to 1.65 dB. The demand for smaller devices has driven the development of compact antennas capable of operating across multiple bands. The main benefits of this antenna include its compact size, enhanced bandwidth, and design simplicity, which is achieved by integrating slots into the patch and introducing a tiny slot etched over the ground plane. The antenna is created using an FR4 material with a thickness of 1.6 mm and dimensions of 25×15 mm². The antenna prototype was fabricated and tested to validate its performance. Simulation optimization reveals that the antenna operates with a gain of 0.9–1.65 dB and a bandwidth of (472–1130 MHz). The design also achieves a VSWR of less than 1.3 and a radiation efficiency between 74% and 78%. The performance enhancement of the reconfigurable antenna was fine-tuned utilizing microwave solvers in both computer simulation technology (CST) and advance design system (ADS).

This is an open access article under the [CC BY-SA](#) license.



Corresponding Author:

Tejal Tandel

Department of Electronics Engineering, Madhuben and Bhanubhai Institute of Technology (MBIT)

School of Engineering, CVM University

Gujarat, India

Email: tbandel@mbit.edu.in

1. INTRODUCTION

As wireless communication technology progresses, there is an increasing demand for flexible and efficient antennas, particularly for sub-6 GHz applications, especially for sub-6 GHz applications [1], which has significantly increased. Reconfigurable antennas, unlike traditional ones, can adapt their operating parameters including frequency, polarization, and radiation characteristics in response to varying environments and system demands. Reconfigurable antennas are broadly categorized into electrically, optically, physically, and smart-material-based tunable designs. The current trends in frequency reconfigurable antennas focus on their versatility and integration into advanced communication systems. The integration of deployable and reconfigurable antennas [2] will pave the way for innovative advancements in antenna design for space communications. This flexibility allows reconfigurable antennas to provide high performance in a variety of scenarios, enhancing the efficiency, reliability, and versatility within the scope of wireless communication [3]. Designing a frequency-reconfigurable antenna for the sub-6 GHz spectrum involves several challenges, including achieving a broad tuning range within the band, ensuring consistent

radiation efficiency across different frequencies, handling the complexity of switching mechanisms, and balancing size limitations with performance needs, particularly given the large wavelengths at these frequencies. With the rollout of 5G technology, the need for antennas [4] that can support multiple frequency bands and varying operational conditions has become essential.

The antenna design [5] described utilizes a hexagonal structure to optimize multi-band performance. It incorporates a coplanar waveguide (CPW) feed, which ensures effective power transfer and reduced loss. Another design [6] includes an I-shaped antenna capable of resonating at two frequency bands, making it ideal for applications like WiMAX and WLAN. Additionally, a compact, reconfigurable T-shaped planar antenna [7] is designed for portable use, providing efficient and adaptable performance across multiple frequency bands. A Vivaldi antenna mentioned in the literature [8] operates over a wide frequency range and employs a slot-line feed to enhance reconfigurability and performance. By embedding a pair of PIN diodes into horizontal and vertical strips, in design [9] enables several reconfigurable frequency ranges within the 3 GHz to 10 GHz range.

Choukiker and Behera [10] frequency reconfigurable wide band kotch snowflake fractal antenna is analyzed. The frequency reconfiguration for ultra high frequency (UHF) frequency range achieved employing RF PIN diodes along with Lumped element like capacitors and inductors. Nguyen-Trong *et al.* [11] discusses a dual-band, compact monopole antenna that employs varactor diodes to adjust frequencies. The pre-fractal structure described in [12] allows for greater miniaturization while maintaining high performance, effectively expanding the surface area without requiring additional space, through optimizing both size and functionality. Furthermore, Chaouche *et al.* [13] introduces a CPW to provide a reconfigurable antenna with a crescent-patterned fractal design. It employs RF PIN diodes, resistors, and inductors to enable adjustable switching across eight frequency ranges, spanning from 1.46 to 6.15 GHz. A CPW-fed triangular patch antenna [14], linked to two distinct serpentine stubs through two PIN diodes, is proposed to achieve radiation across up to eight different frequency bands and a wideband spectrum. The design [15]-[17] demonstrates a frequency reconfigurable antenna achieved using PIN diodes.

Based on the literature survey, the following critical factors have been drawn, which inspire the present work: the need for minimizing the problem of narrow bandwidth and low gain in conventional antennas, and a compact antenna that can work with 5G bands. Therefore, we aim to design and develop a compact, wideband, frequency-reconfigurable antenna operating in the sub-6 GHz spectrum, improving performance and flexibility for modern wireless communication systems. This manuscript presents several innovative features, including:

- The proposed antenna consists of a simple geometrical configuration, thus leading to significantly reduced fabrication error. Designing a compact antenna that incorporate PIN diodes while maintaining high performance across various frequency bands remains a challenge.
- Dual-band functionality, which provides a gain of up to 1.9 dB at 3.9 GHz and covers a bandwidth of 1130 MHz.
- The antenna can resonate at two separate frequency bands, making it ideal for 5G fixed wireless applications and other wireless networking requirements.

2. ANTENNA DESIGN

This section outlines the fundamental structure and design concept in reference to the proposed stacked T-shaped antenna. This geometry allows easy integration of switches (e.g., PIN diodes) for tuning. A modified conductive ground plane is utilized to enhance radiation efficiency and optimize radiated patterns in the far field. In simulations, frequency reconfiguration is managed using lumped RLC components, and a PIN diode is incorporated in the fabrication process to enable frequency reconfigurability. Figure 1 depict the proposed antenna from the top and bottom perspectives, respectively with dimensions of 15×25 mm². The antenna is fabricated on a FR-4 substrate with a relative dielectric constant 4.4, thickness 1.6 mm and loss tangent of 0.02. The length of the partial ground (L_g) is optimized as shown in Figures 1(a) and 1(b). It also changes the resonant frequency. But to achieve the desired frequency with the same antenna dimension, ground plane length is truncated. The parametric values of the optimized stacked T shape are mentioned in Table 1.

The dimensions of the monopole antenna, such as length (L) and width (W) are determined using well-established equations based on transmission line approach [18].

$$L = \frac{c}{4fr\sqrt{\epsilon_{eff}}} - \Delta L \quad (1)$$

By considering fringing fields, the effective permittivity can be obtained using the (2).

$$\epsilon_{\text{eff}} = \frac{\epsilon_r + 1}{2} - \frac{\epsilon_r - 1}{2} \frac{1}{\sqrt{1 + 12 \frac{h}{w}}} \quad (2)$$

In this context, “ c ” denotes the speed of light in a vacuum, while “ ΔL ” signifies the extension length “ ϵ_{eff} ” stands for the effective permittivity, “ ϵ_r ” denotes relative dielectric constant, “ h ” indicates the antenna thickness, and “ w ” represents substrate width.

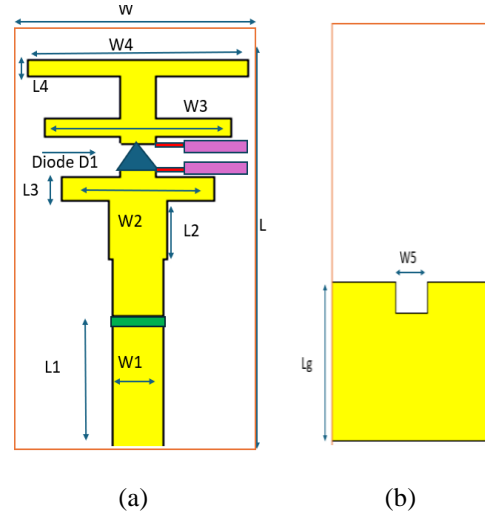


Figure 1. Designed antenna configuration of (a) top view (shows red inductor, purple biasing strips, and green capacitor) and (b) ground level view

Table 1. Antenna design parameters and dimensions

| Parameters | W | L | Lg | W5 | L1 | W4 |
|------------|----|-----|----|-----|------|----|
| Value (mm) | 15 | 25 | 10 | 3 | 12.5 | 13 |
| Parameters | W1 | L2 | W2 | L3 | W3 | L4 |
| Value (mm) | 3 | 3.5 | 9 | 1.5 | 11 | 1 |

2.1. Equivalent circuit modeling of the proposed monopole antenna

For a single resonant frequency, a monopole antenna fed via a microstrip line can be represented by an equivalent circuit composed of a parallel RLC network—comprising a resistor (R), an inductor (L), and a capacitor (C). The proposed antenna, however, operates at two distinct resonant frequencies. Therefore, two separate resonant modes are considered in the development of its equivalent lumped element model for both ON and OFF states. The design utilizes a single parallel RLC circuit to represent the antenna's behavior. This equivalent lumped circuit model was developed using Keysight advance design system (ADS) software. The values of the lumped components are determined using the following (3)–(5) [18].

The computer simulation technology (CST)-simulated input impedance (Z_{11}) of the antenna, including both real and imaginary parts for the ON and OFF states, is illustrated in Figure 2—specifically in Figures 2(a) and 2(b), respectively. Table 2 summarizes the corresponding real and imaginary impedance values, along with the resonant frequencies and the calculated inductance (L) and capacitance (C) values, derived from (3) and (4). The value of real part of the impedance i.e. resistance (R), can be obtained directly from the real impedance plot.

$$L = \frac{\text{img}(z_{11})}{2\pi f} \quad (3)$$

$$C = \frac{1}{(2\pi f)^2 L} \quad (4)$$

$$f = \frac{1}{2\pi\sqrt{LC}} \quad (5)$$

The equivalent circuit, derived from the calculated R, L, and C values, is modeled and analyzed in ADS, as illustrated in Figures 3(a) and 3(b) for the ON and OFF states, respectively. The simulated results of the lumped equivalent circuit are compared with the electromagnetic (EM) simulation results in Figure 4—specifically in Figures 4(a) and 4(b). To ensure optimal impedance matching, the resistor values R4 and R5 are tuned accordingly. Both are powerful electromagnetic simulation tools, but they differ in methodologies, assumptions so both of the simulator results are very.

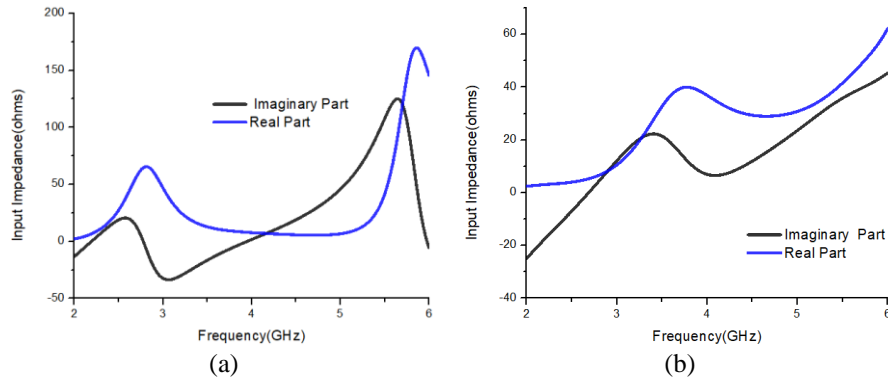
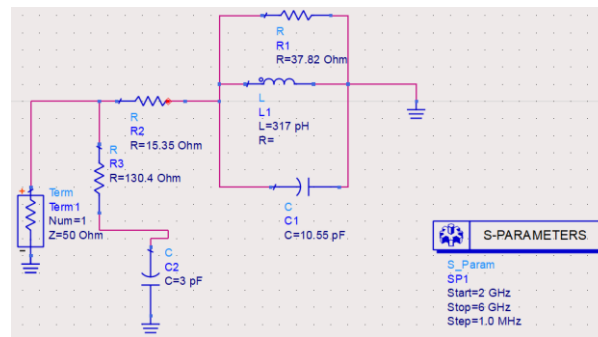


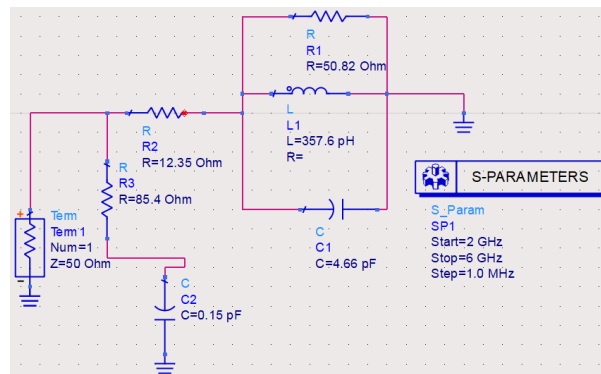
Figure 2. Real and imaginary values of input impedance (Z_{11}) obtained from CST (a) ON state and (b) OFF state

Table 2. Equivalent circuit parameters (R, L, and C) for the proposed antenna

| Resonant frequency (GHz) | Real (Z_{11}) in ohm | Img (Z_{11}) in ohm | L (pH) | C (pH) |
|--------------------------|--------------------------|-------------------------|--------|--------|
| ON state (at 2.7) | 37.82 | 5.48 | 317 | 10.55 |
| OFF state (at 3.9) | 50.82 | 8.76 | 357.6 | 4.66 |



(a)



(b)

Figure 3. Equivalent lumped circuit representation of the proposed patch antenna developed in ADS (a) ON state and (b) OFF state

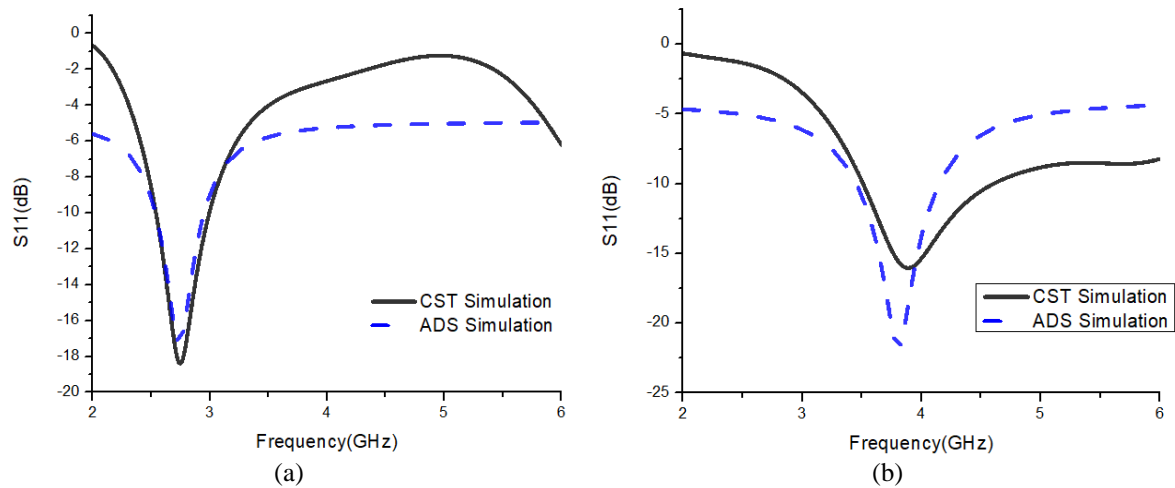


Figure 4. Comparison of reflection coefficient results obtained from ADS and CST simulations of (a) diode ON and (b) diode OFF

2.2. Novelty in design optimization

The steps involved in the design process are illustrated in Figure 5, while Figure 6 showcases the corresponding results related to return loss characteristics. It is clear from the figure that the final two steps lead to better performance compared to the other structures. A tuning phase was conducted to enhance the antenna's performance regarding impedance, operating bandwidth and signal return loss. When the rectangular patch is added to the second stage on top of the radiator, the return loss response experiences a further enhancement in the lower band. In forth step, a rectangular slot of different lengths and width is added including PIN diode. As shown in Figure 5, this step results in an increased reflection coefficient due to imperfect matching. In step 5, a double T-shape is introduced on a rectangular patch, tuned to a frequency of 3.3 GHz (from 3.08 GHz to 3.8 GHz). In step 6, there is simultaneously a resonance at 2.7 GHz (from 2.53 GHz to 2.99 GHz) with complete T-stacked. The foundation of the suggested antenna is rooted in stage 6. After finalizing the structure, the effect of the dimensions of the slots was studied through a parametric analysis. To match impedance, the feeding line width (W_1) is fixed at 3 mm. L_g is the length of the metallic ground plane (10 mm).

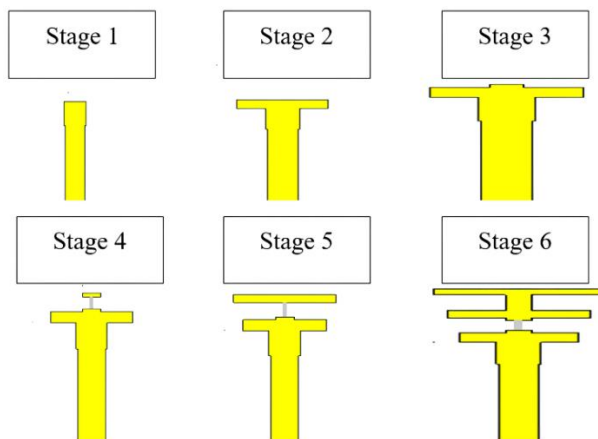


Figure 5. Different design stages for studying the designed antenna

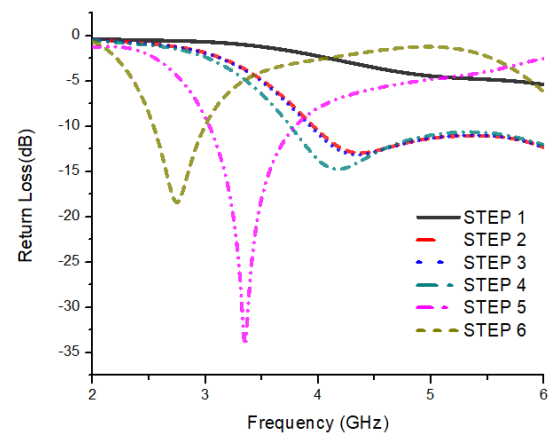


Figure 6. Return loss of the design assessment

2.3. Analysis of parametric results

The parametric evaluation of the presented antenna, depicted in Figure 7, shows how changes in specific parameters influence the resonant frequency. The parametric evaluation of the presented antenna, shown in Figure 7, demonstrates how changes in specific parameters influence the resonant frequency. Figure 7(a) shows that variation in parameter L_2 affects the resonant frequency. Reducing the length of slot leftward-shifting of resonance but after $L_2=3$ mm impedance matching start reducing so to achieve a resonant frequency close to 2.7 GHz, parameter L_2 is set to 2 mm. Then, the antenna is modified to resonate at 2.7 GHz by deflectable ground structure. Similarly, Figure 7(b) shows that variations in W_4 affect the resonant frequency, with a chosen value of W_4 set to 14 mm to obtain the targeted frequency. With reducing value of W_2 , resonance frequency is reducing and shifting in left most. As the length of top slot reduces, reflection coefficient plot shifts to the right side with minor changes in resonance frequency. Figures 7(c) and 7(d) illustrate that adjusting the parameters W_2 and L_4 influences the resonant frequency. To achieve the desired resonant frequency, W_2 is set to 7.5 mm, and L_4 is adjusted to 1 mm with reflection coefficient of 17 dB and 18 dB respectively. All the parameters of proposed design optimized together and summarized in Table 1.

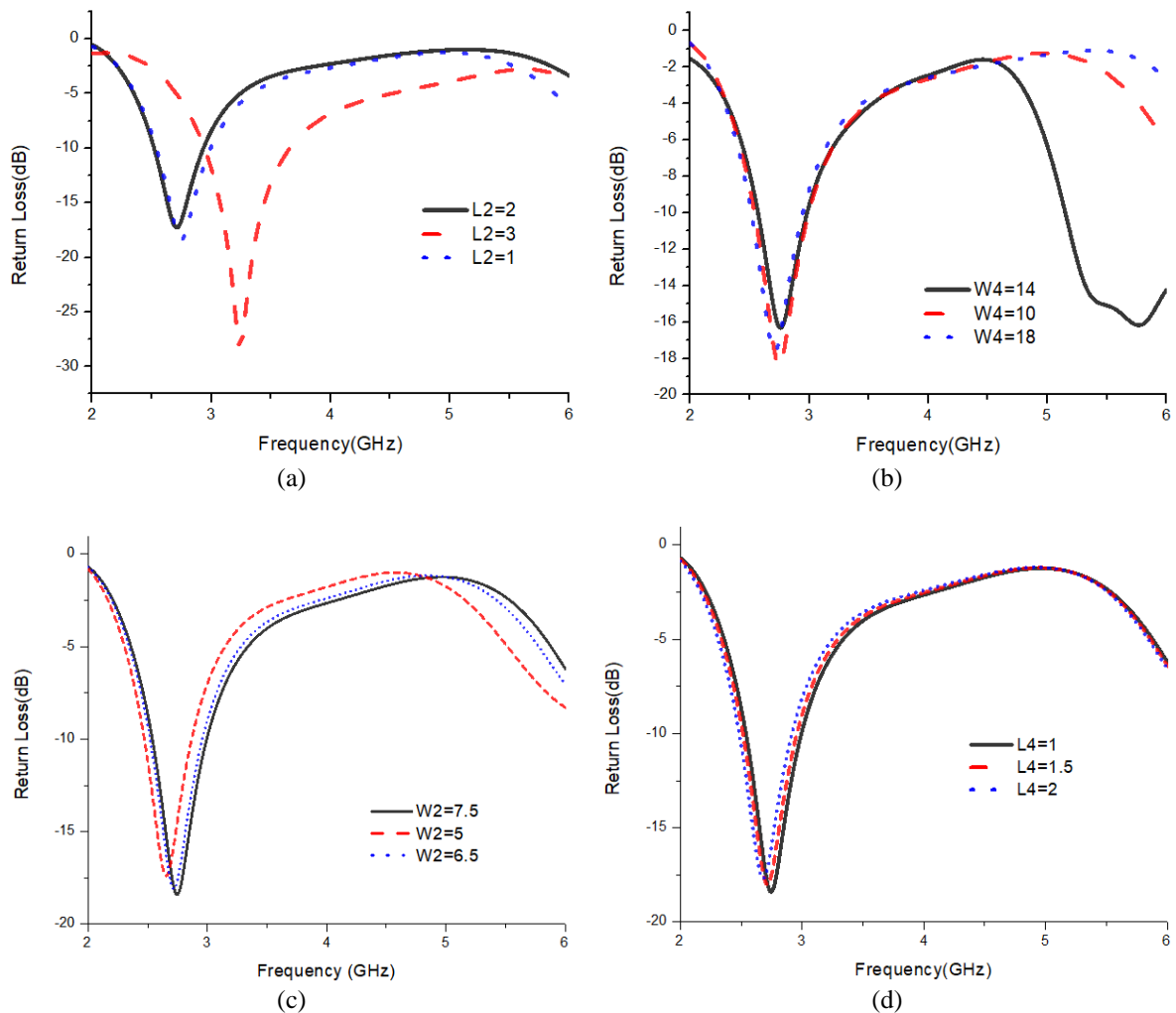


Figure 7. Parametric analysis for (a) impact of variations in L_2 , (b) impact of variations in W_4 , (c) impact of variations in W_2 , and (d) impact of variations in L_4

2.4. Switching technique

PIN diodes, specifically the BAR50-02V model, are utilized for switching within the RF spectrum. Figure 8(a) shows the circuit schematic of the PIN diode in its active (ON) and inactive (OFF) states. In simulation environment, PIN diode is designed as lumped RLC boundary as shown in Figure 8(b). DC bias

voltage exceeds a given threshold, the diode is equivalent in function to a series R-L network whereas DC bias voltage is below the required threshold, diode can be modeled as a parallel combination of RC in series with inductance. The PIN diode is modeled by using the equivalent circuit of particular PIN diode in CST software. To validate the antenna's frequency reconfiguration, the Skyworks BAR50-02V PIN diode has been integrated into the measurement setup. As per its datasheet, this diode is represented in CST using the following parameters: $R_f=3\text{ Ohm}$, $L=0.6\text{ nH}$, $R_p=5\text{K Ohm}$, and $C=0.1\text{ pF}$.

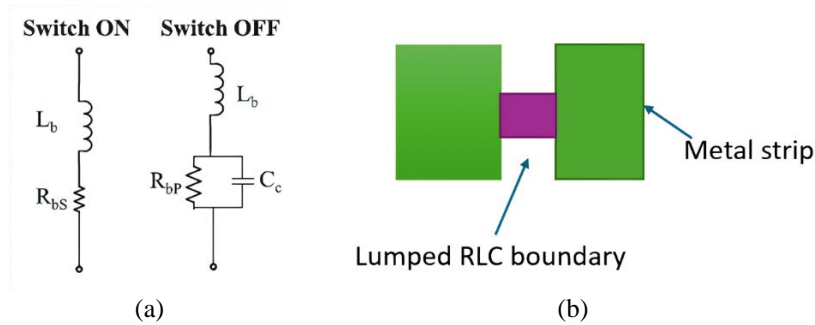


Figure 8. Representation of the PIN diode (a) circuit schematic and (b) CST simulation model

Figure 9(a) demonstrates the biasing circuit for the PIN diode, which was modeled using CST's schematic circuit designer to assess its effect on the designed antenna. To attenuate the steady-state signal from attaining the antenna's RF signal source, a 10pF ceramic capacitor is added to the antenna feedline, and bias lines are etched to link 12nH inductors, effectively isolating the DC and RF waves. The values of the RF choke and DC blocking capacitor are carefully chosen to ensure that the operation of the antenna remains unaffected. A 3 V bias voltage, supplied by two AA alkaline batteries, is applied to the PIN diode. As a part of measurement setup, the bias control circuit is placed on the antenna's front planeto enable real-time functioning of the PIN structure. Figure 9(b) shows the control circuit for the PIN diode biasing arrangement. Jumper wires, commonly used in mobile phone repairs, are employed in the fabricated structure to provide a biasing to the PIN diode.

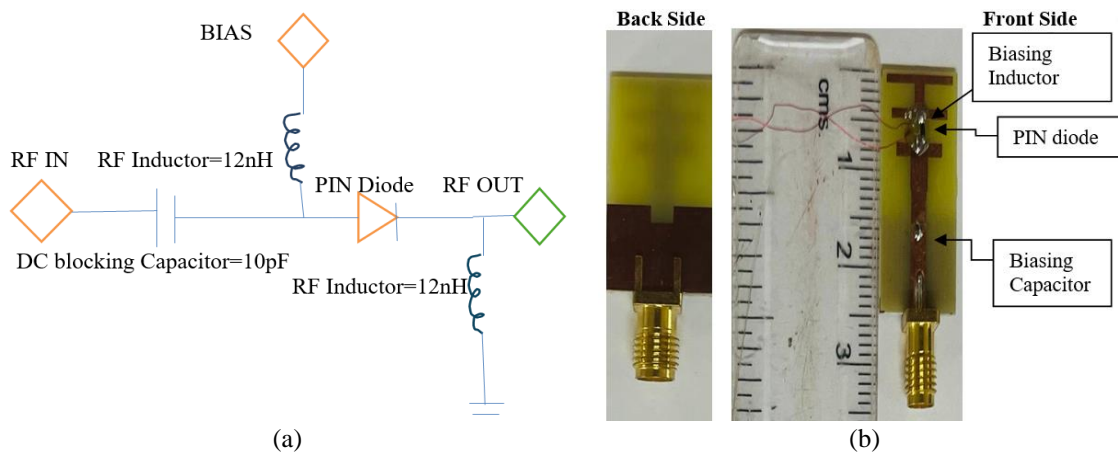


Figure 9. Overview of the proposed antenna setup for (a) biasing configuration of the PIN diode and (b) fabricated prototype of the proposed antenna

3. RESULT ANALYSIS

The evaluated antenna features a stacked T-shaped design, which was simulated using CST software and subsequently fabricated for testing. Return loss measurements were conducted for the different active (ON) and inactive (OFF) PIN operational states using an Agilent vector network analyzer (VNA) (9-15 GHz) shown in Figure 10.

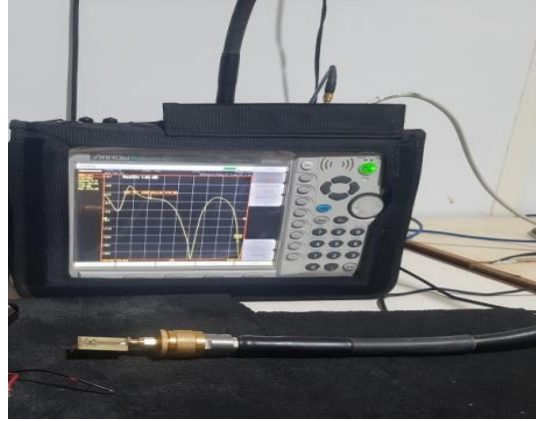


Figure 10. The measurement setup for reflection coefficient

In the designed antenna, frequency switching is achieved by toggling the PIN junction diode between its ON and OFF mode, as represented in Table 3. This switching mechanism allows for the desired frequency adjustments. Discrepancies between CST/ADS and measurements are attributed to substrate tolerance, PIN diode package parasitics and bias-network stubs, as well as chamber positioning/cable effects, all consistent with the stated uncertainty bounds.

Table 3. States of switching

| Switching condition | Resonant frequency (GHz) |
|---------------------|--------------------------|
| Diode ON | 2.7 |
| Diode OFF | 3.9 |

A strong agreement is observed between the simulated and experimental results, as shown in Figure 11 specifically in Figures 11(a) and 11(b), for the ON and OFF states of the proposed antenna. The small discrepancies observed can be attributed to the loss caused by the insertion of the PIN diode (BAR50-02 V) according to the specifications. The first passband band is operating from 2.53 GHz to 2.99 GHz having a centre frequency of 2.7 GHz, with overall impedance bandwidth of 472 MHz. The second passband is operating from 3.51 GHz to 4.64 GHz having centre frequency of 3.9 GHz. The overall impedance bandwidth in this case is 1130 MHz. The table highlights the minor differences between experimental and simulated results. Table 4 provides a comparison of the performance of our proposed antenna with that of previously published studies from recent years.

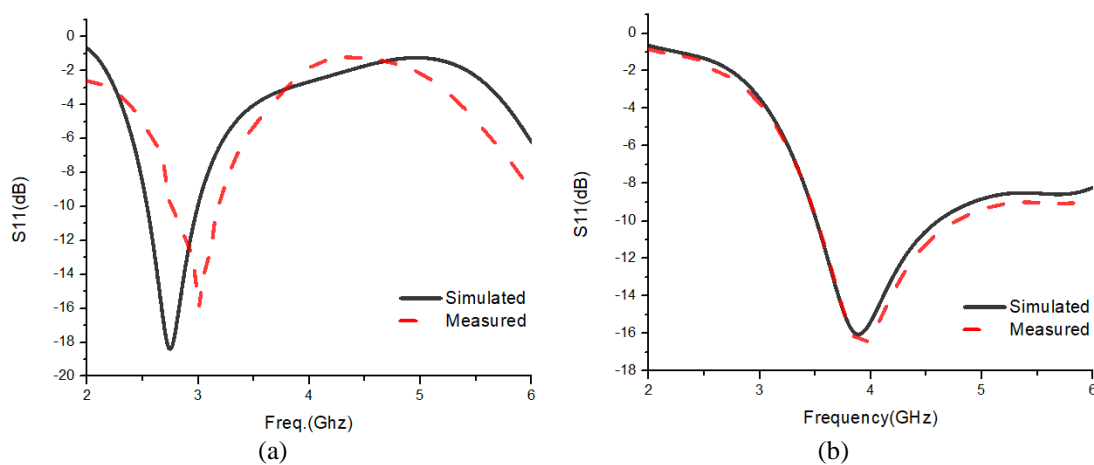


Figure 11. Comparison of experimental and simulated reflection coefficient of the proposed design (a) ON mode and (b) OFF mode

Table 4. Simulated versus experimental results comparison of frequency reconfigurable antenna

| Switched mode | Frequency range (GHz) | | Bandwidth (MHz) | | Gain (dB) | Rad. efficiency (%) |
|---------------|-----------------------|--------------|-----------------|--------------|-----------|---------------------|
| | Simulated | Experimental | Simulated | Experimental | Simulated | |
| Diode ON | 2.53-2.99 | 2.74-3.19 | 472 | 450 | 0.9 | 74 |
| Diode OFF | 3.51-4.64 | 3.59-4.79 | 1130 | 1200 | 1.65 | 78 |

Figure 12 shows the measured and simulated antenna gain and efficiency versus operating frequency for OFF state. The results demonstrate a comparison between experimental measurements and simulation data, highlighting the performance of the antenna across the frequency spectrum. Although the gain and efficiency are relatively modest, this may be attributed to factors such as compact antenna dimensions, substrate losses, and the inherent insertion loss of the PIN diode used for reconfiguration. The antenna was subjected to measurement within a calibrated anechoic chamber to assess its far-field radiation characteristics shown in Figure 13. The fabricated prototype was positioned on a rotating platform, facing a wideband horn antenna placed 1 m away. The diode was regulated using a DC source set at 3 V according to the datasheet specifications. Experimental testing, including radiation pattern analysis was conducted in an anechoic chamber.

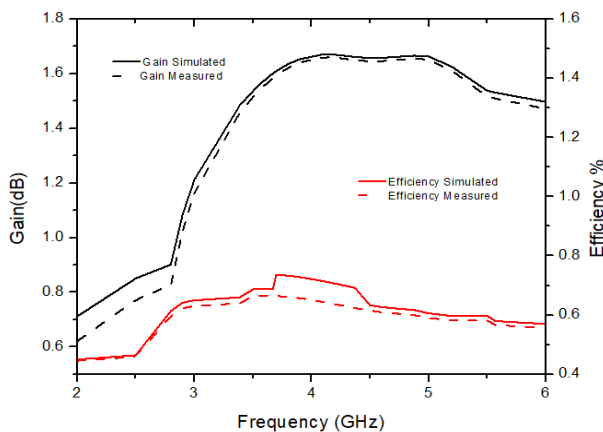


Figure 12. Gain and efficiency plot of stacked T-shaped antenna during OFF state

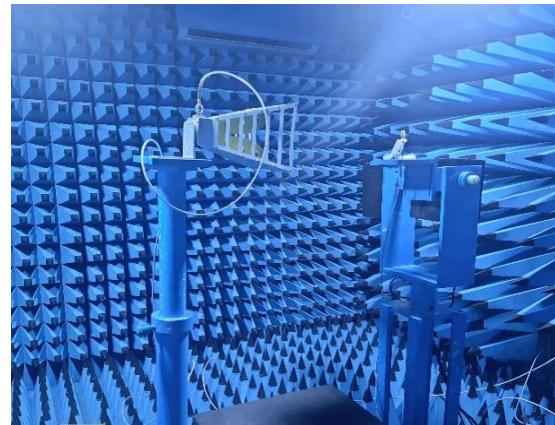


Figure 13. The proposed configurable antenna's far-field setup

These results show a good deal of validation for experimental results. Current distribution on the surface over the antenna's structure is examined in CST Microwave Studio at frequencies of 2.7 GHz and 3.9 GHz, as illustrated in Figures 14(a) and (b). The resonance dimensions of the fabricated antenna are examined using the transmission line approach. At the lower frequency of 2.7 GHz, the surface current intensity is highest along the top slot of stacked T-shaped antenna, which improves radiation at this frequency. Very less surface current is flowing below PIN diode of monopole antenna. At 3.9 GHz, a smaller portion of the rectangular form (slot below the PIN diode) contributes to radiate in the upper frequency range.

In Figure 15 simulated and measured radiation patterns of the proposed antenna: Figures 15(a) H-plane and 15(b) E-plane at 2.7 GHz and 3.9 GHz. For all possible switching cases the antenna possesses monopole like radiation pattern in principle E-plane ($\text{PHI}=0^\circ$) while a nearly omnidirectional radiation pattern is observed in H-plane ($\text{PHI}=90^\circ$) at all resonating frequencies, as depicted in Figure 12. As observed in Figure 15, the evaluated E-plane field distribution of the antenna follows a "Figure of 8" shape. In Figure 16 gain performance of the proposed antenna in two modes: Figures 16(a) ON state showing an optimal gain of 0.9 dB at 2.7 GHz in the far-field region, and 16(b) OFF state achieving a maximum gain of 1.65 dB at 3.9 GHz.

Table 5 presents analysis of the proposed work with prior studies, emphasizing size, reconfiguration type, and the total actuators applied for frequency reconfiguration. There was minor frequency shifting in fabricated and simulated results due to soldering and fabrication loss. The relative dimensions are determined based on λ , at the lowest operating frequency of the specific antenna. Although the work reported in [19], [20] had supports more than 2 operational bands but with larger electrical size, less gain and more than 1 PIN diode used. Clearly, the designed antenna is more compact and utilizes minimal actuators than the alternative antenna models discussed.

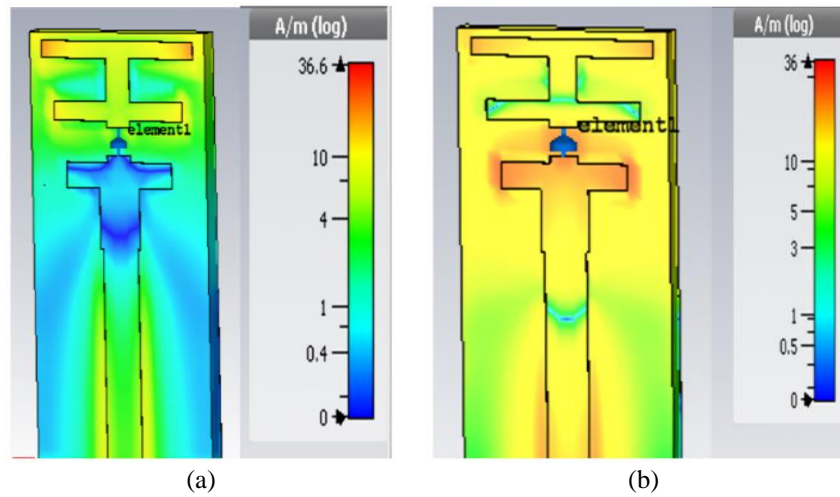


Figure 14. Current distribution on the surface at (a) 2.7GHz and (b) 3.9GHz

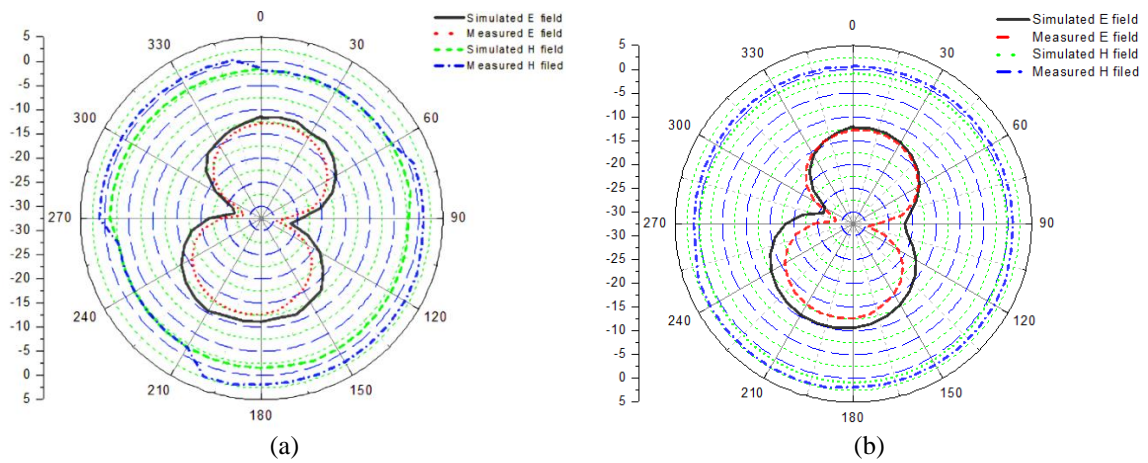


Figure 15. Simulated radiation of proposed antenna at various frequencies for various switching state at (a) 2.7 GHz and (b) 3.9 GHz

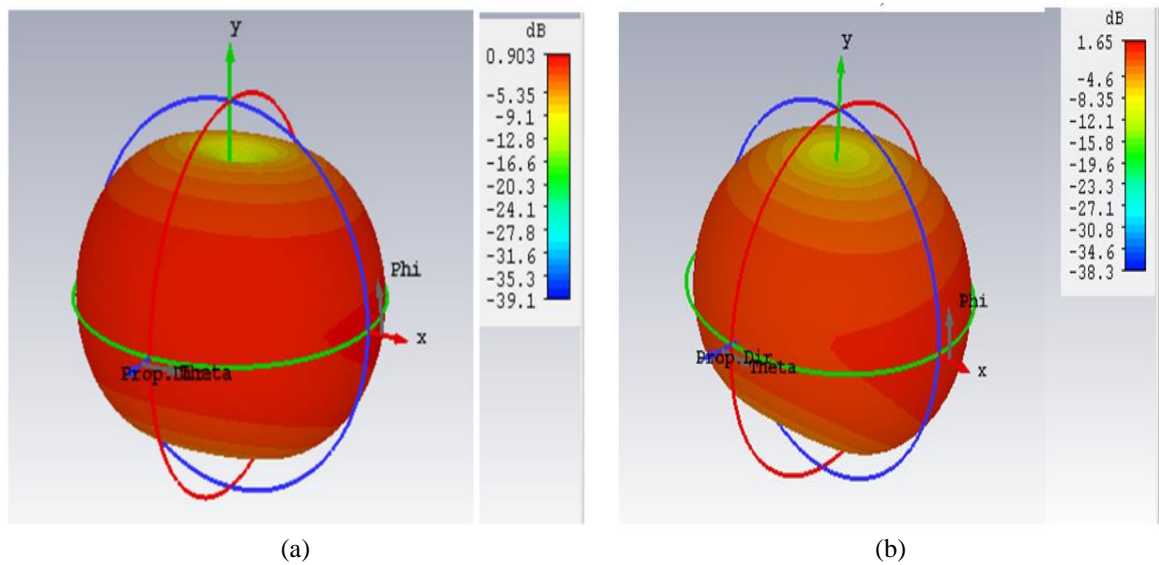


Figure 16. Peak gain at (a) 2.7GHz and (b) 3.9GHz

Table 5. Proposed antennas relative to other reported studies

| Reference | Dimensions (mm ²) | Resonance frequency (GHz) | Actuators | Relative dimensions (λ) | Bandwidth (MHz) | Simulated gain (dB) |
|-----------|-------------------------------|---------------------------|------------------|-----------------------------------|-----------------|---------------------|
| [21] | 31×42.04 | 3.6,11,11.8,13.9 | 2 PIN diode | 0.37×0.51 | 300-1000 | 1.7-2.2 |
| [19] | 25×28 | 2.9,3.1,5.45,7.50,7.7,8.1 | 2 PIN diode | 0.24×0.27 | 1080-5300 | -4.3 |
| [22] | 35×40 | 2.45,3.80,5.2 | 1 switch | 0.33×0.29 | 330-1250 | -1.86 |
| [23] | 37×35 | 2.3,4.2,4.3,1 | 2 PIN diode | 0.25×0.23 | 200-920 | 1.44-2.2 |
| [24] | 53×35 | 2.45,3.5,5.2 | 1 PIN diode | 0.43×0.28 | 147-1820 | 1.7-3.41 |
| [20] | 16×33 | 2.1,2.4,3.5,4.1,4.8,5.2 | 3 PIN diode | 0.11×0.23 | 196-2003 | 0.3-1.31 |
| [25] | 22×21 | 1.08,1.12,1.16 | 1 Varactor diode | 0.082×0.078 | 1.00-1.15 | -2.15 |
| This work | 15×25 | 2.7,3.8 | 1 PIN | 0.14×0.23 | 470-1130 | 0.9-1.65 |

4. CONCLUSION

In this work, a novel stacked T-shaped frequency reconfigurable monopole antenna has been constructed and tested experimentally validated in this article. A single PIN diode facilitates frequency reconfiguration approach simplifies design complexity, reduces manufacturing cost, and can be readily integrated into portable consumer electronics. The antenna is constructed to resonate at 2.7 GHz (for mobiles broadband deployment) and 3.9 GHz (for 5G fixed wireless access) in different switching states. Designed with a compact form factor suitable for portable devices, this antenna offers several advantages over previous designs, including a compact size, cost-effective, lightweight construction, and ease of fabrication. The gain values achieved are appropriate for the intended applications. In the future work, the frequency reconfigurable antenna can be Integration with MIMO systems.

ACKNOWLEDGMENTS

The research was performed and carried out at the ELARC-Electromagnetic and Antenna Research Centre, which is operated for BVM Engineering College, Vallabh Vidya Nagar-Gujarat-India by Electronics Engineering department.




REFERENCES

- [1] F. Rahmani, A. Belbachir Kchairi, M. El Bakkali, N. Taher, N. Amar Touhami, and T. E. Elhamadi, "Sub-6 GHz Reconfigurable Beam-Switched Circular Antenna for Wireless Networks," *Arabian Journal for Science and Engineering*, vol. 50, no. 8, pp. 5589–5602, 2025, doi: 10.1007/s13369-024-09445-0.
- [2] C. G. Christodoulou, Y. Tawk, S. A. Lane, and S. R. Erwin, "Reconfigurable antennas for wireless and space applications," *Proceedings of the IEEE*, vol. 100, no. 7, pp. 2250–2261, Jul. 2012, doi: 10.1109/JPROC.2012.2188249.
- [3] M. Zhang, G. Xu, and R. Gao, "Reconfigurable Antennas for Wireless Communication: Design Mechanism, State of the Art, Challenges, and Future Perspectives," *International Journal of Antennas and Propagation*, vol. 2024, no. 1, Jan. 2024, doi: 10.1155/2024/3046393.
- [4] R. J. Beneck *et al.*, "Reconfigurable Antennas: A Review of Recent Progress and Future Prospects for Next Generation," *Progress In Electromagnetics Research*, vol. 171, pp. 89–121, 2021, doi: 10.2528/PIER21081109.
- [5] S. Ullah, I. Ahmad, Y. Raheem, S. Ullah, T. Ahmad, and U. Habib, "Hexagonal shaped CPW Feed based Frequency Reconfigurable Antenna for WLAN and Sub-6 GHz 5G applications," in *2020 International Conference on Emerging Trends in Smart Technologies, ICETST 2020*, Mar. 2020, pp. 1–4, doi: 10.1109/ICETST49965.2020.9080688.
- [6] P. Thanki and F. Raval, "I-shaped frequency and pattern reconfigurable antenna for WiMAX and WLAN applications," *Progress in Electromagnetics Research Letters*, vol. 97, pp. 149–156, 2021, doi: 10.2528/PIERL21021903.
- [7] A. Iqbal, S. Ullah, U. Naeem, A. Basir, and U. Ali, "Design, fabrication and measurement of a compact, frequency reconfigurable, modified T-shape planar antenna for portable applications," *Journal of Electrical Engineering and Technology*, vol. 12, no. 4, pp. 1611–1618, 2017, doi: 10.5370/JEET.2017.12.4.1611.
- [8] S. Chagharvand, M. R. Hamid, M. R. Kamarudin, and J. R. Kelly, "Wide and multi-band reconfigurable Vivaldi antenna with slot-line feed," *Telecommunication Systems*, vol. 65, no. 1, pp. 79–85, May 2017, doi: 10.1007/s11235-016-0213-z.
- [9] T. Khan and M. U. Rahman, "Design of low-profile frequency reconfigurable antenna for multiband applications," *International Journal of Electronics Letters*, vol. 10, no. 1, pp. 30–47, Jan. 2022, doi: 10.1080/21681724.2020.1818836.
- [10] Y. K. Choukiker and S. K. Behera, "Wideband frequency reconfigurable Koch snowflake fractal antenna," *IET Microwaves, Antennas and Propagation*, vol. 11, no. 2, pp. 203–208, Jan. 2017, doi: 10.1049/iet-map.2016.0238.
- [11] N. Nguyen-Trong, A. Piotrowski, and C. Fumeaux, "A Frequency-Reconfigurable Dual-Band Low-Profile Monopolar Antenna," *IEEE Transactions on Antennas and Propagation*, vol. 65, no. 7, pp. 3336–3343, Jul. 2017, doi: 10.1109/TAP.2017.2702664.
- [12] R. Azaro, G. Boato, M. Donelli, A. Massa, and E. Zeni, "Design of a prefractional monopolar antenna for 3.4-3.6 GHz Wi-Max band portable devices," *IEEE Antennas and Wireless Propagation Letters*, vol. 5, no. 4, pp. 116–119, 2006, doi: 10.1109/LAWP.2006.872427.
- [13] Y. B. Chaouche, I. Messaoudene, I. Benmabrouk, M. Nedil, and F. Bouttout, "Compact coplanar waveguide-fed reconfigurable fractal antenna for switchable multiband systems," *IET Microwaves, Antennas and Propagation*, vol. 13, no. 1, pp. 1–8, Jan. 2019, doi: 10.1049/iet-map.2018.5005.
- [14] W. A. Awan *et al.*, "A miniaturized wideband and multi-band on-demand reconfigurable antenna for compact and portable devices," *AEU - International Journal of Electronics and Communications*, vol. 122, p. 153266, Jul. 2020, doi: 10.1016/j.aeu.2020.153266.




- [15] A. Ghaffar, X. J. Li, W. A. Awan, A. H. Nazeri, N. Hussain, and B. C. Seet, "Compact multiband multimode frequency reconfigurable antenna for heterogeneous wireless applications," *International Journal of RF and Microwave Computer-Aided Engineering*, vol. 31, no. 7, Jul. 2021, doi: 10.1002/mmce.22659.
- [16] G. Jin, C. Deng, J. Yang, Y. Xu, and S. Liao, "A new differentially-fed frequency reconfigurable antenna for WLAN and sub-6GHz 5G applications," *IEEE Access*, vol. 7, pp. 56539–56546, 2019, doi: 10.1109/ACCESS.2019.2901760.
- [17] A. Boufrioua, "Frequency Reconfigurable Antenna Designs Using PIN Diode for Wireless Communication Applications," *Wireless Personal Communications*, vol. 110, no. 4, pp. 1879–1885, Feb. 2020, doi: 10.1007/s11277-019-06816-x.
- [18] R. Bansal, *Antenna theory; analysis and design*, 2nd ed., vol. 72, no. 7. 2008, doi: 10.1109/proc.1984.12959.
- [19] S. Mudda, K. M. Gayathri, and M. Mallikarjun, "Wide-Band Frequency Tunable Antenna for 4G, 5G/Sub 6 GHz Portable Devices and MIMO Applications," *Progress In Electromagnetics Research C*, vol. 118, pp. 25–41, 2022, doi: 10.2528/PIERC21112902.
- [20] I. A. Shah *et al.*, "Design and analysis of a hexa-band frequency reconfigurable antenna for wireless communication," *AEU - International Journal of Electronics and Communications*, vol. 98, pp. 80–88, Jan. 2019, doi: 10.1016/j.aeue.2018.10.012.
- [21] S. P. Lavadiya *et al.*, "Low profile multiband microstrip patch antenna with frequency reconfigurable feature using PIN diode for S, C, X, and Ku band applications," *International Journal of Communication Systems*, vol. 35, no. 9, Jun. 2022, doi: 10.1002/dac.5141.
- [22] I. A. Shah, S. Hayat, I. Khan, I. Alam, S. Ullah, and A. Afridi, "A Compact, Tri-Band and 9-Shape Reconfigurable Antenna for WiFi, WiMAX and WLAN Applications," *International Journal of Wireless and Microwave Technologies*, vol. 6, no. 5, pp. 45–53, Sep. 2016, doi: 10.5815/ijwmt.2016.05.05.
- [23] S. Ullah *et al.*, "Frequency reconfigurable antenna for portable wireless applications," *Computers, Materials and Continua*, vol. 68, no. 3, pp. 3015–3027, 2021, doi: 10.32604/cmc.2021.015549.
- [24] S. Ullah, S. Hayat, A. Umar, U. Ali, F. A. Tahir, and J. A. Flint, "Design, fabrication and measurement of triple band frequency reconfigurable antennas for portable wireless communications," *AEU - International Journal of Electronics and Communications*, vol. 81, pp. 236–242, Nov. 2017, doi: 10.1016/j.aeue.2017.07.028.
- [25] M. Al Ahmad, S. Kabeer, A. A. Sanad, and L. J. A. Olule, "Compact single-varactor diode frequency-reconfigurable microstrip patch antenna," *IET Microwaves, Antennas and Propagation*, vol. 15, no. 9, pp. 1100–1107, Jul. 2021, doi: 10.1049/mia2.12117.

BIOGRAPHIES OF AUTHORS



Tejal Tandel    received her B.E. degree from Department of Electronics Engineering, Gujarat University, Gujarat, India in 2008, the M.E. degree from LDEC, Gujarat Technological University, Gujarat, India in 2011 and the Pursuing Ph.D. from CVM University India. She is currently an Assistant Professor at Madhuben and Bhanubhai Institute of Technology engineering college from 2011 till the date. She has more than 14 years of teaching and research experience. Her area of interest includes antenna designing and microwave engineering. She has delivered many expert talks on antenna and wave propagation in various colleges of Gujarat. She has published more than 15 research papers in various journals and international conferences She has organized 5+workshops seminars on antenna designing using CST software/advance instrumentation for the B.E. She has attended as well as organized many STTP. She can be contacted at email: tbandel@mbit.edu.in.



Dr. Samir Trapasiya    received B.E. (electronics and communication) from Saurashtra University in 2003, M.E. (electronics and communication) from D.D.U, Nadiad in 2006. Presently, he is Ph.D. degree from Gujarat Technology University, Ahmedabad in 2018. He has more than 18 years of teaching and research experience. His interests include wireless communication, wireless network, and cross layer optimization has guided 11+ME. Students in their dissertation as well as more than 10 projects B.E. students. He has published more than 20 research papers in various journals and international conferences. He has delivered many expert talks on various domains of wireless communications in various colleges of Gujarat. He has served as reviewer/TPC members of many international conferences. He has organized 30+workshops on LabVIEW/MATLAB /advanced instrumentation for the B.E. as well as M.E. students. He has attended as well as organized many STTP and symposium. He can be contacted at email: samirtrapasiya@gcet.ac.in.